Partitioning of Pyrene-Labeled Phospho- and Sphingolipids between Ordered and Disordered Bilayer Domains

Mirkka Koivusalo,* Joni Alvesalo,* Jorma A. Virtanen,† and Pentti Somerharju*
*Institute of Biomedicine, Department of Biochemistry, University of Helsinki, Helsinki, Finland and †Department of Chemistry, Nanoscience Center, University of Jyväskylä, Jyväskylä, Finland

ABSTRACT Here we have studied how the length of the pyrene-labeled acyl chain (*n*) of a phosphatidylcholine, sphingomyelin, or galactosylceramide affects the partitioning of these lipids between 1), gel and fluid domains coexisting in bovine brain sphingomyelin (BB-SM) or BB-SM/spin-labeled phosphatidylcholine (PC) bilayers or 2), between liquid-disordered and liquid-ordered domains in BB-SM/spin-labeled PC/cholesterol bilayers. The partitioning behavior was deduced either from modeling of pyrene excimer/monomer ratio versus temperature plots, or from quenching of the pyrene monomer fluorescence by spin-labeled PC. New methods were developed to model excimer formation and pyrene lipid quenching in segregated bilayers. The main result is that partition to either gel or liquid-ordered domains increased significantly with increasing length of the labeled acyl chain, probably because the pyrene moiety attached to a long chain perturbs these ordered domains less. Differences in partitioning were also observed between phosphatidylcholine, sphingomyelin, and galactosylceramide, thus indicating that the lipid backbone and headgroup-specific properties are not severely masked by the pyrene moiety. We conclude that pyrene-labeled lipids could be valuable tools when monitoring domain formation in model and biological membranes as well as when assessing the role of membrane domains in lipid trafficking and sorting.

INTRODUCTION

In recent years, evidence has accumulated suggesting that segregated lipid domains, or ''rafts,'' exist in the plasma membrane as well as in some other membranes of eukaryotic cells (Simons and Ikonen, 1997). There is presently a wide interest in membrane rafts and other membrane domains since they are thought to play a crucial role in many important cellular phenomena, like signal transduction and intracellular sorting of membrane proteins and lipids (Brown and London, 2000; Anderson and Jacobson, 2002; Simons and Ehehalt, 2002; Edidin, 2003). The actual lipid composition of rafts is not known, but they are thought to be rich in cholesterol and sphingolipids and therefore to exist in liquid-ordered (l_o) phase in contrast to the liquid-disordered (l_d) phase, a state that most natural glycerophospholipids exist in at physiological temperatures (Ipsen et al., 1987; Sankaram and Thompson, 1990; Vist and Davis, 1990; Almeida et al., 1992; Schroeder et al., 1994, 1998; Ahmed et al., 1997).

The major unresolved issues regarding rafts relate to their composition, size, and lifetime, and whether or not the rafts include both monolayers of the bilayer (Maxfield, 2002; Edidin, 2003; Silvius, 2003). Fluorescent lipid analogs are potentially useful tools to study these issues because of the sensitivity of fluorescence detection and the possibility to use both spectroscopic and microscopic approaches. However, to be useful as a raft probe, the fluorescent analog should partition effectively to the raft domains. Because the lipids in rafts are thought to be conformationally ordered and tightly packed together, one would assume that fluorescent lipids containing a bulky and fairly polar fluorophore in the acyl chain would be largely excluded from rafts. Conversely, probes with long, saturated alkyl/acyl chains are expected to interact favorably with conformationally ordered lipids and thus partition to rafts. These predictions seem to be largely correct as indicated by recent studies (Mesquita et al., 2000; Wang et al., 2000; Wang and Silvius, 2000; Samsonov et al., 2001).

Pyrene lipids have been extensively used to study lateral organization of membranes (reviewed in Pownall and Smith, 1989; Somerharju, 2002). The main reason for this is that an excited pyrene lipid molecule can form excimers upon collision with another pyrene lipid in the ground state, and that the rate of excimer formation is proportional to the local pyrene lipid concentration. The ratio of excimer/monomer fluorescence intensities (*E*/*M*) thus provides information on the lateral distribution and mobility of pyrene lipids in the bilayer (Galla and Sackmann, 1975). Partitioning of pyrene lipids between gel-state and fluid-state (liquid-crystalline) domains has been investigated by recording the *E*/*M* ratio as a function of temperature (Chong and Thompson, 1985; Somerharju et al., 1985; Hresko et al., 1986, 1987; Jones and Lentz, 1986; Ollmann et al., 1987; Viani et al., 1988). In those studies, however, only a single, or few, pyrene lipid species were employed and therefore systematic information

Submitted June 10, 2003, and accepted for publication October 10, 2003.

Address reprint requests to Pentti Somerharju, Institute of Biomedicine, Dept. of Biochemistry, University of Helsinki, Biomedicum, Room C205b, P. O. Box 63, 00014 University of Helsinki, Finland. Tel.: 358-9-191-25410; Fax: 358-9-191-25444; E-mail: pentti.somerharju@helsinki.fi.

Abbreviations used: BB-SM, bovine brain sphingomyelin; DOPC, dioleoylphosphatidylcholine; DPPC, dipalmitoylphosphatidylcholine; DSPC, distearoylphosphatidylcholine; MLV, multilamellar vesicle; l_d, liquid-disordered; l_o, liquid-ordered; Pyr_nPC, 1-palmitoyl-2-pyrenylacyl-phosphatidylcholine (n = number of aliphatic carbons in the labeled acyl chain); Pyr_nSM, pyrenylacylsphingomyelin; $Pyr_nGalCer$, pyrenylacylgalactosylceramide; 7-SLPC, 1-palmitoyl-2-(7-doxyl)-stearoyl-phosphatidylcholine; 12-SLPC, 1-palmitoyl-2-(12-doxyl)-stearoyl-phosphatidylcholine.

0006-3495/04/02/923/13 $2.00

on the effect of the acyl chain length or the lipid backbone/polar headgroup structure on the partitioning behavior is lacking. Second, in those earlier studies the bilayer matrix usually consisted of a single saturated phospholipid species and was thus quite different from natural membranes. Therefore, additional studies with more natural-like systems are needed to determine how pyrene lipids partition between different membrane domains and whether they could be used to study raft formation and properties. Such information is also crucial when pyrene lipids are employed to investigate lipid trafficking and sorting in cells (Masserini et al., 1990; Agmon et al., 1991; Kasurinen and Somerharju, 1995; Tanhuanpää and Somerharju, 1999; Heikinheimo and Somerharju, 2002).

Here we have studied the effect of the length of the labeled acyl chain of Pyr_nPC, Pyr_nSM, and $Pyr_nGalCer$ (n = the number of carbons in the labeled acyl chain) on the partitioning of the parent lipid between 1), gel and fluid domains coexisting in BB-SM and BB-SM/spin-labeled PC bilayers or 2), between l_d and l_o domains in BB-SM/spin-labeled PC/cholesterol bilayers. The partitioning was determined based either on *E/M* versus temperature curves or quenching of the pyrene monomer fluorescence by spin-labeled PC molecules. The key result is that whereas the pyrene lipids with a short labeled chain strongly preferred the fluid/l_d domains, those with a long chain had a markedly higher affinity for gel/l_o domains. The lipid headgroup/backbone had a modest effect on partitioning.

MATERIALS AND METHODS

Lipids and other reagents

BB-SM, dioleoylphosphatidylcholine (DOPC), 1-palmitoyl-2-(7-doxyl)-stearoylphosphatidylcholine (7-SLPC), and 1-palmitoyl-2-(12-doxyl)-stearoylphosphatidylcholine (12-SLPC) were purchased from Avanti Polar Lipids (Alabaster, AL). Sphingosylphosphorylcholine and lysogalactosylceramide were obtained from Larodan (Malmö, Sweden) and the other chemicals from Sigma (St. Louis, MO). The 1-palmitoyl-2-pyrenylacylphosphatidylcholine (Pyr_nPC) species were synthesized as described previously (Somerharju et al., 1987). Pyrenylacylsphingomyelins (Pyr_nSM) and pyrenylacylgalactosylceramides ($Pyr_nGalCer$) were synthesized essentially as described elsewhere (Ahmad et al., 1985) and purified on a Licrosphere 100 DIOL column (5-μm particle size, 250 × 4.6 mm; Alltech, Deerfield, IL) using a solvent system described previously (Silversand and Haux, 1997). All lipids were >98% pure and were stored in chloroform/methanol (4:1, v/v) <−20°C.

Preparation of multilamellar liposomes

To prepare multilamellar vesicles (MLV), the lipids were mixed in chloroform and the solvent was evaporated under a nitrogen stream at 55°C to 60°C and samples were then kept in a vacuum desiccator for 3 to 16 h. The lipids were dispersed in 20 mM Tris-HCl, 1 mM EDTA, and 150 mM NaCl, at pH 7.4 (TEN) buffer for fluorometry, and 0.5 mM phosphate, 1 mM EDTA, 50 mM NaCl, and 0.02 mg/ml NaN_3, at pH 7.4 (PEN) buffer for calorimetry. The samples containing Pyr_nPC or Pyr_nSM were hydrated at 65°C and the samples containing $Pyr_nGalCer$ at 85°C. The samples for *E/M* ratio versus temperature measurements and calorimetry were first incubated at the hydration temperature for 10 min in the dark, vortexed for 1 min, and again incubated at the hydration temperature for 2 min. This sequence was repeated twice, after which the samples were allowed to cool to room temperature and kept at 4°C for at least 16 h before the measurement. For fluorometric analysis the total lipid concentration was adjusted to 16.1 μM and for calorimetry to 1.7–3.3 mM (with 2 mol % of a pyrene lipid). For the fluorescence quenching assays, MLVs with a total lipid concentration of 50 μM (with 0.3 mol % pyrene lipid) were prepared as described previously (Wang et al., 2000; Wang and Silvius, 2000). The samples were incubated for 15 min at 45°C, 1 min at 75°C, vortexed twice for 10 s, incubated for 15 min at 45°C, and then allowed to cool to the desired temperature at which they were kept for 2–4 h before the measurement.

Fluorometry

The *E/M* versus temperature measurements were performed on a PTI Quantamaster (Lawrenceville, NJ), fluorescence spectrophotometer equipped with two emission monochromators and detectors. The excitation wavelength was set to 345 nm (bandwidth 2 nm), and the emission wavelengths to 378 nm (bandwidth 4.5 nm) and 475 nm (bandwidth 22 nm), for the pyrene monomer and excimer fluorescence, respectively. The temperature in the cuvette was regulated with a Braun Thermomix UB (Melsungen, Germany), temperature bath under computer control and was recorded with a probe placed in the cuvette. The samples were maintained at 10°C for 10 min and then heated to 80°C at a rate of 1°C/min. The fluorescence quenching assays were performed on a Varian Cary Eclipse fluorometer (Varian, Cary, NC) equipped with a thermostated cuvette holder. The excitation (345 nm) and emission (378 nm) bandwidths were as described above. After incubating the samples for the quenching assays at the temperature of measurement for 2–4 h, they were placed into the thermostated cuvette, incubated in the dark for 30 s at the same temperature, and fluorescence intensity was determined using a signal integration time of 5 s. The quenching curves were not significantly altered if the preincubation at the temperature of measurement was extended to 10 h, in agreement with previous studies (Wang et al., 2000; Wang and Silvius, 2000). Other control experiments also indicated that the systems studied were at or close to an equilibrium.

Differential scanning calorimetry

The MLVs dispersed in PEN buffer were degassed for 10 s in a sonicating bath and then introduced into the sample cell of a 6100 Nano II differential scanning calorimeter (Calorimetry Sciences, American Fork, UT). The reference cell contained an equal volume of the PEN buffer. The temperature was maintained at 10°C for 10 min and then raised to 80°C at the rate of 1°C/min.

Other methods

The molecular species of BB-SM were quantified by electrospray mass-spectrometry as described previously (Koivusalo et al., 2001). The concentrations of lipid stocks were determined based on a phosphate assay (Bartlett and Lewis, 1970).

RESULTS

E/M versus temperature plot as an indicator of gel/liquid-domain partitioning of pyrene lipids

Previous studies have indicated that partitioning of pyrene-labeled lipids between fluid and gel bilayer domains can be studied by measuring the pyrene excimer/monomer (*E/M*)

emission intensity ratio as a function of temperature (Galla and Sackmann, 1975; Somerharju et al., 1985; Hresko et al., 1986, 1987; Jones and Lentz, 1986). Whereas in those studies homogenous, saturated PC species were used as the matrix lipid, we chose to use BB-SM which is a mixture of several molecular species containing 16:0, 18:0, 20:0, 22:0, 24:1, and 24:0 fatty acyl residues as determined by mass-spectrometry. As shown in Fig. 1 *A*, BB-SM undergoes a gel-to-fluid phase transition between ~15 and 47°C, in agreement with earlier data (Barenholz et al., 1976; Calhoun and Shipley, 1979). This transition actually consists of at least three subtransitions as indicated by the complex peak shape and deconvolution (Fig. 1 *A*). The presence of several transitions is obviously due to the acyl chain heterogeneity of BB-SM. The subtransitions at ~36°C and ~41°C may be attributed to domains consisting of species with long and saturated acyl chains, whereas the transition at ~26°C probably derives from the melting of the species with shorter and/or more unsaturated chains. Notably, the BB-SM liposomes used for the calorimetry also contained 2 mol % of Pyr_6PC to allow direct comparison with *E/M* versus temperature curves (see below). Very similar calorimetric curves were obtained if Pyr_6PC was replaced with any other Pyr_nPC/SM/GalCer species or if no pyrene lipid was included (data not shown).

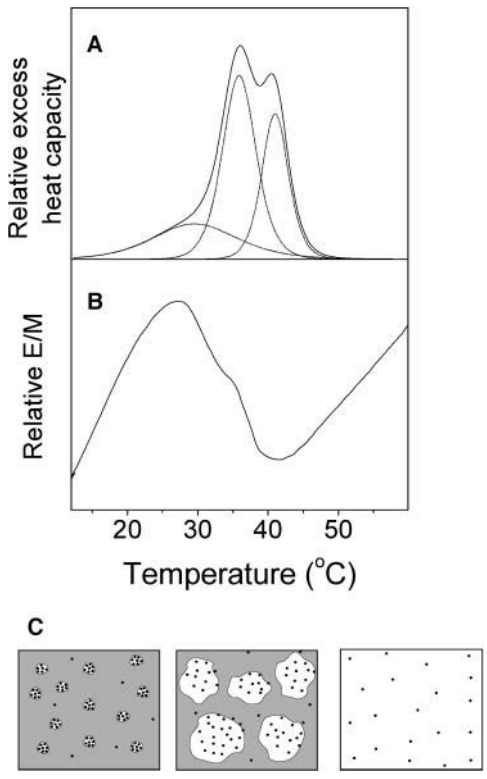

FIGURE 1 Relationship between *E/M* versus temperature curves and phase behavior of short-chain pyrene lipids. Multilamellar vesicles consisting of 98 mol % BB-SM and 2 mol % of Pyr_6PC lipid were prepared and the heat capacity (*A*) and the *E/M* ratio (*B*) were measured as a function of temperature as detailed in Materials and Methods. *C* relates the *E/M* ratio to the distribution of Pyr_6PC below T_m (*left panel*), at the phase transition region (*middle panel*), and above T_m of BB-SM (*right panel*). The shaded areas represent gel and the open areas fluid domains, whereas the solid dots represent Pyr_6PC molecules.

Fig. 1 *B* shows an *E/M* versus temperature plot obtained for Pyr_6PC/BB-SM MLVs. Similarly to the earlier studies (Somerharju et al., 1985; Hresko et al., 1986, 1987; Jones and Lentz, 1986), we interpret this plot as follows (cf. Fig. 1 *C*). When the BB-SM bilayer is initially cooled to a low temperature, the Pyr_6PC molecules cluster because of their low solubility in gel-state BB-SM domains (*far left panel* in Fig. 1 *C*). These clusters most probably also contain some low-melting, i.e., unsaturated/short-chain BB-SM molecules, which probably explains why only a relatively modest increase in excimer formation occurs upon probe clustering. The exclusion of Pyr_6PC from the BB-SM gel domains can be attributed to a poor fit (perturbation) of the bulky pyrene moiety into the tightly packed lipids in such domains (see Discussion). Upon heating, *E/M* gradually increases until the gel-to-liquid phase transition of BB-SM is reached. At this point, *E/M* decreases abruptly due to a gradual disappearance of the Pyr_6PC cluster domains upon melting of the matrix lipid (*middle panel* of Fig. 1 *C*). Any further increase in temperature results in a monotonous increase in *E/M* due to increasing lateral diffusion of the pyrene lipid molecules fully dispersed in the fluid BB-SM matrix (*far right panel* of Fig. 1 *C*). Consistent with this interpretation, the cooling curves fully coincided with the heating curves (data not shown).

The *E/M* versus temperature curves obtained for each Pyr_nPC species ($n = 6$–14) are shown in Fig. 2 *A*. Clearly, the length of the pyrene-labeled chain has a remarkable effect on the shape of the curve. The abrupt decrease of *E/M* observed for Pyr_nPC in the phase transition region of BB-SM upon heating became less evident with increasing chain length and disappeared when $n = 12$. For $Pyr_{14}PC$ even an increase in *E/M* was observed. The shape of the curves strongly suggests that partitioning of Pyr_nPC to the gel domains becomes increasingly favorable as n increases.

Pyr_nSM behaved similarly to Pyr_nPC (Fig. 2 *B*); i.e., the longer the labeled acyl chain, the smaller is the deflection in *E/M* curve, thus indicating that partitioning to the gel phase domains increases systematically with n. Careful comparison of the curves in Fig. 2, *A* and *B*, indicates that each Pyr_nSM may partition somewhat less to the gel domains than Pyr_nPC with equal n. We also tested how the length of the labeled acyl chain affects the partitioning of a glycosphingolipid derivative, $Pyr_nGalCer$ (Fig. 2 *C*). Also in this case the plots clearly indicate that partitioning to the gel domains increases systematically with increasing chain length. However, the curves deviated again somewhat from those obtained for Pyr_nPC, thus supporting the notion that partitioning of pyrene-labeled lipids between gel and fluid domains is not determined merely by the length of the labeled acyl chain (see below).

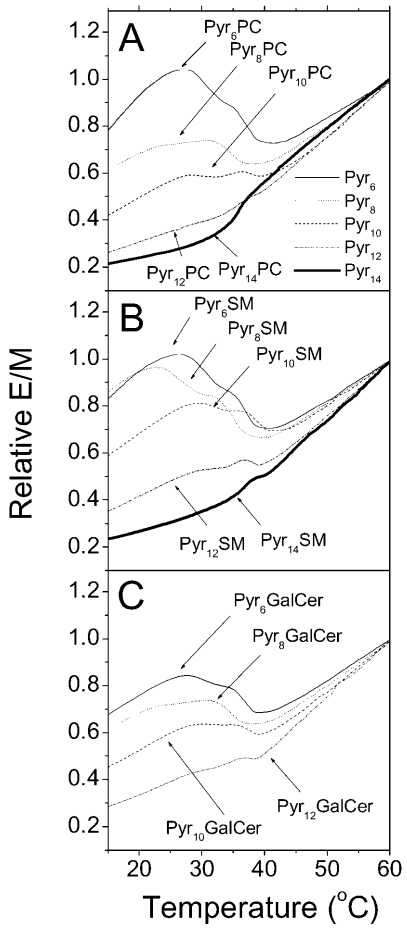

FIGURE 2 Excimer/monomer intensity ratio versus temperature curves for different pyrene lipids incorporated in BB-SM bilayers. Two mol percent of the indicated pyrene lipid was incorporated in multilamellar BB-SM liposomes and *E*/*M* was determined as a function of increasing temperature as described in Materials and Methods. (*A*) Pyr_nPC, (*B*) Pyr_nSM, and (*C*) $Pyr_nGalCer$ (n = 6, 8, 10, 12, or 14). The experiment was repeated three times with essentially identical results. Practically identical curves were also obtained in cooling runs.

Quantitative analysis of pyrene lipid distribution between gel and liquid domains in BB-SM bilayers based on *E*/*M* versus temperature plots

To assess more quantitatively the gel/liquid partition of the different pyrene-labeled lipids an empirical model was constructed (see Appendix 1). Notably, only two subtransitions, i.e., those centered at ~36°C and ~28°C (Fig. 1 *A*), were taken into account when applying this model here. The transition at ~41°C was neglected simply because none of the probes seemed to respond significantly to this subtransition (Fig. 2). The most probable explanation for this lack of response is that the pyrene-labeled lipids do not partition significantly to the corresponding gel domains probably consisting mainly of the long-chain and saturated SM species. A low affinity of pyrene lipids containing the rather bulky pyrene moiety for such domains with tightly packed acyl chains would not be unexpected.

Fig. 3 shows the experimental and modeled *E*, *M*, and *E*/*M* versus temperature curves for a short- and long-chain Pyr_nPC species (Pyr_6PC and $Pyr_{14}PC$). As can be seen, a reasonable fit was obtained in each case. Similar results were obtained for all other pyrene lipids (not shown). The gel versus liquid partition coefficients obtained from those fits are plotted as a function of labeled chain length in Fig. 4. The model provides two partition coefficients: one for partitioning between the fluid domains and the gel domains with T_m of ~36°C ($K_{g/f(36°C)}$), and the other for partitioning between the fluid domains and gel domains with T_m of ~28°C ($K_{g/f(28°C)}$). As would be expected from the data shown in Fig. 2, the probes with a short labeled chain partitioned mainly to the fluid domains at 36°C, whereas those with a long chain partitioned equally to both types of domains, or even slightly preferred the gel domains. The long-chain $Pyr_nGalCer$ derivatives (n = 10 or 12) partitioned somewhat more to the gel domains than the corresponding Pyr_nPC and Pyr_nSM derivatives (Fig. 4 *A*). This indicates, that beside the lipid backbone, the headgroup also has an effect on pyrene lipid partitioning between gel and fluid domains. Interestingly, the pyrene lipids partitioned nearly equally between the fluid and gel domains with T_m of ~28°C independent of the length of

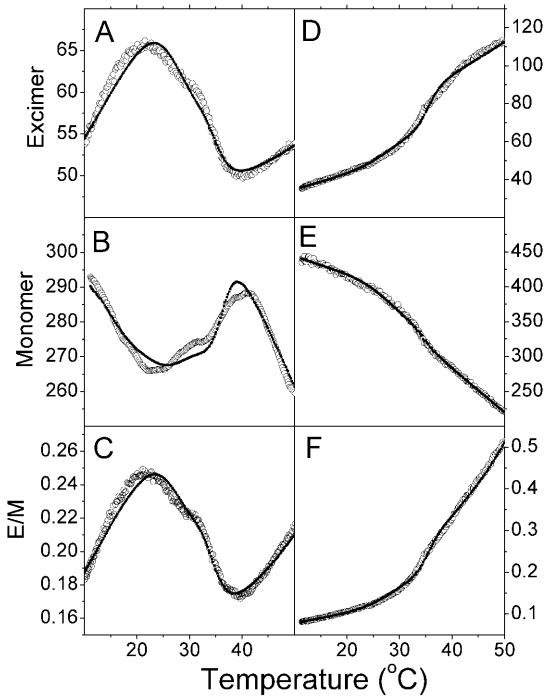

FIGURE 3 Experimental and modeled excimer, monomer, and excimer/monomer versus temperature curves for Pyr_6PC and $Pyr_{14}PC$. Experimental curves (*open circles*) obtained for liposomes containing 2 mol % of Pyr_6PC (*A–C*) or $Pyr_{14}PC$ (*D–F*) are shown together with curves (*dotted line*) obtained by fitting of an empirical model (Appendix 1) to the data. It is important to note that a global fitting protocol was used here, i.e., the temperature, cooperativity, and maximal fractional area of the individual transitions were forced to be identical for all Pyr_nPC, Pyr_nSM, and $Pyr_nGalCer$ species.

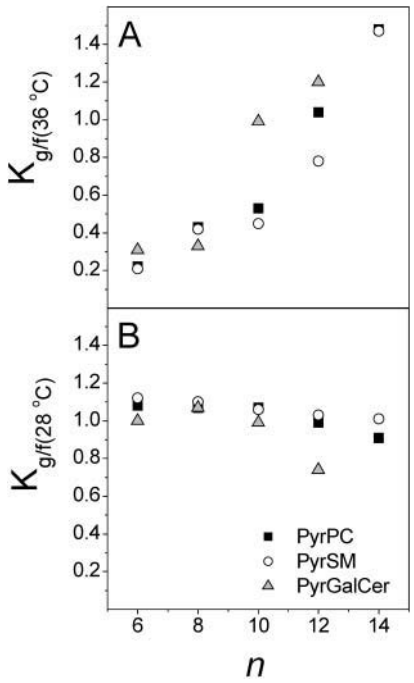

FIGURE 4 Gel/fluid partition coefficients for pyrene lipids obtained by modeling of the excimer and monomer fluorescence versus temperature curves. The gel/fluid partition coefficients were obtained by fitting of the model described in Appendix 1 to the experimental curves as shown in Fig. 3 and are plotted as a function of pyrenylacyl chain length (n). (A) Partition coefficients at 36°C ($K_{g/f(36°C)}$). (B) Partition coefficients at 28°C ($K_{g/f(28°C)}$). The error in the partition coefficients was tested with selected samples by determining how systematic variation of the partition coefficient affects the fit quality. Already when the partition coefficient obtained by fitting was changed by 10%, the modeled curve deviated clearly more from the experimental one than what was the typical deviation between experimental curves from different experiments. Based on this finding, we estimate that the error in the partition coefficients is <10%.

the pyrene-labeled chain and other structural details (Fig. 4 *B*). The cause for such structure independent partitioning could be that these low-melting domains probably consist of BB-SM species with a short and/or unsaturated acyl chain and are thus less ordered and more accommodative than the higher melting domains.

In line with the present results, making use of the *E/M* ratio Jones and Lentz calculated that $Pyr_{10}PC$ partitions seven times more to fluid DOPC-rich domains than to coexisting solid DPPC-rich domains (Jones and Lentz, 1986). Another, qualitative study also indicated that $Pyr_{10}PC$ partitions preferentially to the fluid domains in neat DPPC bilayers (Hresko et al., 1986).

Reliable information on the lateral distribution of pyrene-labeled lipids can be obtained from the *E/M* versus temperature plots only if the pyrene lipid does not cluster significantly in the fluid matrix (Hresko et al., 1987). To study this, *E/M* versus temperature plots were measured for all Pyr_nPC, Pyr_nSM, or $Pyr_nGalCer$ species present at a concentration of 2 mol % in DOPC bilayers. *E/M* increased smoothly with temperature at least to 90°C in each case (data not shown). This suggests that pyrene lipids do not have a significant tendency to cluster in a fluid bilayer; otherwise one would expect to see deviations in the *E/M* versus temperature curve due to melting of the clusters. We also measured the *E/M* ratio for representative pyrene lipids (Pyr_6PC, Pyr_6SM, $Pyr_6GalCer$, $Pyr_{10}PC$, $Pyr_{10}SM$, $Pyr_{10}GalCer$, $Pyr_{14}PC$, and $Py_{14}SM$) versus their concentration (0–10 mol %) in BB-SM bilayers at 50°C. The plots were essentially linear and coincided independent of the headgroup/backbone structure when n was equal (data not shown). Collectively, these results strongly suggest that none of pyrene lipids have any significant tendency to segregate in fluid bilayers at the concentrations used in this study.

Partitioning of pyrene lipids between gel and liquid domains in BB-SM/7-SLPC bilayers as deduced from fluorescence quenching

Earlier studies have demonstrated that partitioning of a fluorescent probe between fluid and gel-like membrane domains can be determined by incorporating the probe into bilayers consisting of a quencher lipid (having a spin-labeled or brominated acyl chain and closely mimicking natural unsaturated PC species) with a low T_m and of an unlabeled lipid with a high T_m, e.g., BB-SM (London and Feigenson, 1981a,b; Huang et al., 1988; Spink et al., 1990; Wang et al., 2000; Wang and Silvius, 2000, 2003). Whereas 12-SLPC has been generally used as the quencher lipid (Ahmed et al., 1997; Wang et al., 2000; Wang and Silvius, 2000; Xu and London, 2000), we chose to use 7-SLPC, inasmuch as this species quenched pyrene lipid fluorescence equally independent of the length of the pyrene-labeled chain in homogenous fluid bilayers (see below), whereas for 12-SLPC significant differences were found (data not shown). The gel-to-liquid phase transition temperature of 7-SLPC was ~8°C as determined by differential scanning calorimetry (our unpublished data). Thus this lipid is in the fluid state at 15°C, the temperature at which the partitioning experiments were carried out.

We first studied the quenching of Pyr_6PC and $Pyr_{14}PC$, i.e., species with a short or a long labeled chain in homogenous, fluid bilayers consisting of DOPC and 7-SLPC. As can be seen in Fig. 5 *A*, the quenching curves obtained for these lipids are essentially superimposable, thus indicating that the pyrene lipid fluorescence is quenched equally by 7-SLPC independent of the length of the pyrene-labeled chain in the absence of domain segregation. Such chain-length independent quenching, which is a prerequisite for obtaining reliable partitioning information in segregated bilayers (Wang et al., 2000), was also observed for other lipids studied, namely Pyr_6PC, $Pyr_{14}PC$, Pyr_6SM, and $Pyr_{14}SM$, in BB-SM/7-SLPC bilayers at 50°C, i.e., when the entire bilayer is in the fluid state (data not shown).

Fig. 5 *B* shows the quenching curves obtained for Pyr_nPC in BB-SM/7-SLPC bilayers at 15°C, a temperature at which

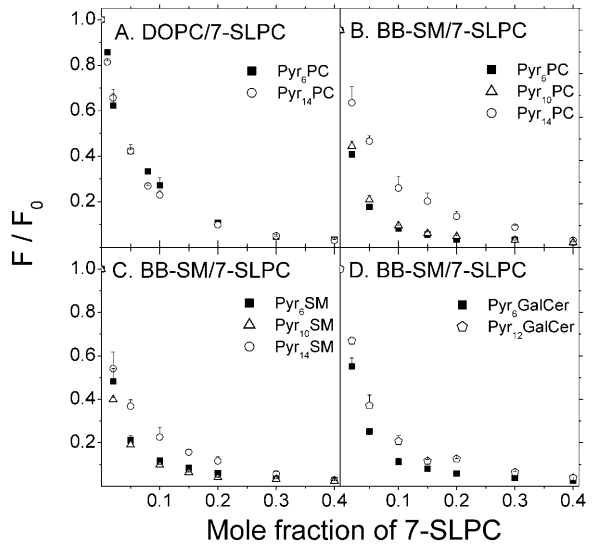

FIGURE 5 Analysis of pyrene lipid partition between coexisting gel and fluid domains as determined by pyrene fluorescence quenching. Multilamellar liposomes containing 0.3 mol % of the indicated pyrene lipid and 0–100 mol % of 7-SLPC, a quencher of pyrene fluorescence, were prepared and the pyrene monomer fluorescence intensity was determined at 15°C as detailed in Materials and Methods. (*A*) Pyr_6PC and $Pyr_{14}PC$ in DOPC/7-SLPC bilayers, (*B*) Pyr_6PC, $Pyr_{10}PC$, and $Pyr_{14}PC$ in BB-SM/7-SLPC bilayers, (*C*) Pyr_6SM, $Pyr_{10}SM$, and $Pyr_{14}SM$ in BB-SM/7-SLPC bilayers, and (*D*) $Pyr_6GalCer$ and $Pyr_{12}GalCer$ in BB-SM/7-SLPC bilayers. Data is shown only up to 7-SLPC mole fraction of 0.4 since complete quenching of each pyrene lipid was observed at higher mole fractions. Each data point represents an average from two to three experiments with three replicate samples. The error bars indicate the standard deviation.

BB-SM-rich gel domains coexist with fluid domains consisting mainly of 7-SLPC over a wide composition range. In contrast to the homogenous bilayers discussed above, the quenching was significantly dependent on the length of the pyrene-labeled chain, i.e., Pyr_6PC and $Pyr_{10}PC$ were quenched more efficiently than $Pyr_{14}PC$. This indicates that the former species partition significantly less to the BB-SM gel domains than the latter one. Analogously, Pyr_6SM and $Pyr_{10}SM$ were quenched more efficiently than $Pyr_{14}SM$ (Fig. 5 *C*) and $Pyr_6GalCer$ more efficiently than $Pyr_{12}GalCer$ (Fig. 5 *D*; $Pyr_{14}GalCer$ was not available, therefore the Pyr_{12} species was used instead). The data clearly indicate that the length of the labeled chain plays an important role in partitioning of the pyrene-labeled lipids between the fluid and gel domains in BB-SM/7-SLPC bilayers. London and Feigenson have previously constructed a model which allows one to determine quantitatively the partitioning of a fluorescent probe between co-existing gel and fluid domains from quenching data (London and Feigenson, 1981b). However, this model is valid only when the quenching is static, i.e., for probes with a relatively short (few nanoseconds) fluorescence lifetime (London and Feigenson, 1981b). The fluorescence lifetime of pyrene lipids in bilayers is >100 ns (Sassaroli et al., 1995), which allows diffusional quenching to take place as well. To account for this, an empirical model was constructed to analyze pyrene lipid partitioning (see Appendix 2). This model assumes that 1), the quenching can be either static or dynamic (diffusional) and 2), the quencher can be either a single quencher lipid molecule or a domain consisting (mostly) of the quencher lipid. Quenching by these two entities are characterized by specific quenching constants, i.e., k_{mon} and k_{dom}, respectively. The value of k_{mon} can be determined for each lipid from quenching at low quencher concentrations ($<\sim$1.5 mol %), i.e., when the bilayer is homogenous. Knowing the value of k_{mon} then allows one to determine both the gel/fluid partition coefficients of the probes as well as k_{dom} which in turn can be used to estimate the average size of the quencher lipid domains. The fitting results indicate that the pyrene lipids with a Pyr_6 or Pyr_{10} acyl chain species strongly prefer the liquid domains, independent of the headgroup or backbone structure (Fig. 6). The Pyr_{14} species appear to partition more to the gel domains than the shorter chain species, albeit they also prefer the fluid domains. A very small value ($\sim$0.04) was obtained for k_{dom} from which one can deduce (see Appendix 2) that the quencher domains are quite large, i.e., consist minimally of several hundreds of lipid molecules.

Partitioning of pyrene lipids between liquid-disordered and liquid-ordered domains coexisting in BB-SM/7-SLPC/cholesterol bilayers

Partitioning of the pyrene lipid between l_o and l_d domains was assessed by varying the quencher lipid content in phospholipid fraction while maintaining the cholesterol content of the bilayer constant (33 mol %). Based on earlier data, BB-SM/cholesterol-rich l_o-domains are present in such bilayers at 37°C when the BB-SM mole fraction is $\sim$0.05–0.85 (Ahmed et al., 1997; Wang et al., 2000; Wang and Silvius, 2000). However, contrary to expectations, only minor differences in quenching between the Pyr_6 and Pyr_{14} species were observed at this temperature (data not shown), which has also been observed for different indolyl-labeled

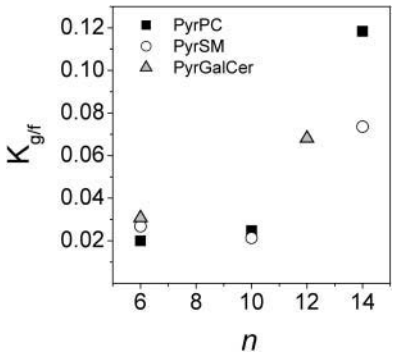

FIGURE 6 Gel/fluid partition coefficients pyrene lipids. The partition coefficients ($K_{g/f}$) were obtained by fitting an equation given in Appendix 2 to the quenching data in Fig. 5, *B–D*.

lipids (Wang and Silvius, 2003). This could be due to the long excited state lifetime of pyrene as well as the small size and/or lifetime of the BB-SM-rich l_o domains at this temperature. We therefore measured the samples at 25°C where the l_o domains are expected to be significantly larger and more stable. The basic characteristics of l_o and l_d domains at this temperature should, however, be similar to those at 37°C as shown for similar systems (cf. Silvius, 1992).

The quenching curves obtained for Pyr_6PC, $Pyr_{10}PC$, and $Pyr_{14}PC$ in BB-SM/7-SLPC/cholesterol bilayers at 25°C are shown in Fig. 7 *A*. Pyr_6PC is quenched significantly more efficiently than either $Pyr_{10}PC$ and $Pyr_{14}PC$, thus indicating that this short-chain species partitions significantly less to l_o domain than those with a longer chain. Interestingly, the curves obtained for $Pyr_{10}PC$ and $Pyr_{14}PC$ cross at 7-SLPC mole fraction of ~0.2–0.3, indicating that partitioning of the pyrene lipids is critically dependent on the position of the pyrene in the bilayer as well as the composition of the coexisting domains. The SM and GalCer derivatives behaved similarly to Pyr_nPC, i.e., the short-chain species appeared to partition less into l_o domains than the long-chain ones (Fig. 7, *B* and *C*). However, the $Pyr_{14}SM$ and $Pyr_{12}GalCer$ species were less quenched at low 7-SLPC mole fractions than $Pyr_{14}PC$, indicating that they partition more to the BB-SM-rich domains than the PC derivative. As a control, we also determined quenching of Pyr_6PC and $Pyr_{14}PC$ in DOPC/7-SLPC/cholesterol bilayers in which no domain segregation should exist (Ahmed et al., 1997; Wang et al., 2000). The quenching curves (Fig. 7 *D*) were virtually identical for the two probes, thus indicating that the intrinsic efficiency of pyrene lipid quenching by 7-SLPC is independent of the length of the pyrene-labeled chain also in the presence of cholesterol.

Due to the complexity of this ternary system, it is not feasible to obtain absolute partition coefficients from the quenching data. However, it is possible to obtain *relative* partition coefficients (Wang et al., 2000). Although this generally requires that a fluorescent species is available that partitions exclusively to l_d domains, this is not the case for the pyrene lipids since they are fully quenched in 7-SLPC domains (Fig. 7). Using *the slope method* of Wang et al. (2000) we determined the relative $K_{lo/ld}$ values for the different pyrene lipids using $Pyr_{12}GalCer$ as the reference. As shown in Fig. 8 the length of the pyrene-labeled chain has a significant effect on Pyr_nPC partitioning, $Pyr_{10}PC$ showing the highest affinity for the l_o domains. However, when *the ratio method* of Wang et al. (2000) was used, the $K_{lo/ld}$ value obtained for $Pyr_{14}PC$ was similar or even higher than that for $Pyr_{10}PC$ at low 7-SLPC mole fractions, as expected from the data in Fig. 7. In case of Pyr_nSM, $K_{lo/ld}$ increased monotonously and only modestly with n, whereas a more significant chain-length dependency was observed for $Pyr_nGalCer$.

As a control, we also determined quenching of a triacylglycerol which contains two oleoyl chains in addition to a Pyr_{10}-acyl chain, and is thus expected to partition largely to the l_d domains (Wang et al., 2000). The shape of the quenching curve obtained for this lipid is indeed consistent

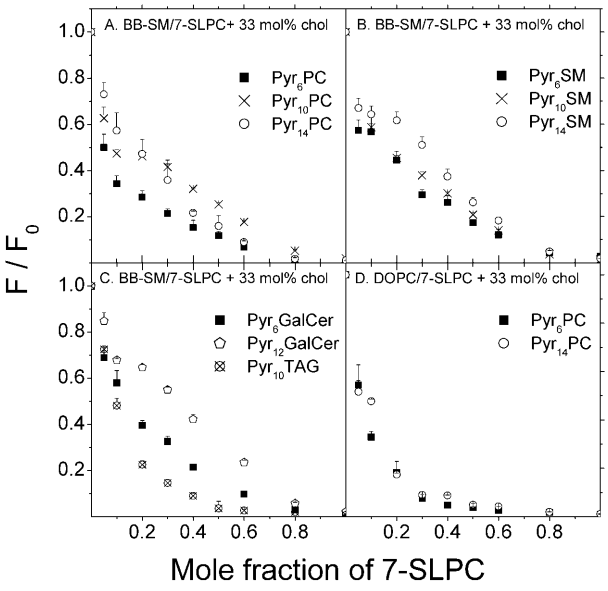

FIGURE 7 Analysis of pyrene lipid partition between coexisting liquid-ordered and liquid-disordered domains as determined by fluorescence quenching. Multilamellar DOPC/7-SLPC/cholesterol (33 mol %) or BB-SM/7-SLPC/cholesterol (33 mol %) liposomes containing the indicated mole fractions of 7-SLPC in the nonsterol fraction were prepared and the fluorescence intensity was measured as detailed in Materials and Methods. (*A*) Pyr_6PC, $Pyr_{10}PCm$, and $Pyr_{14}PC$ in BB-SM/7-SLPC/cholesterol bilayers, (*B*) Pyr_6SM, $Pyr_{10}SM$, and $Pyr_{14}SM$ BB-SM/7-SLPC/cholesterol bilayers, (*C*) $Pyr_6GalCer$, $Pyr_{12}GalCer$, and $Pyr_{10}TAG$ in BB-SM/7SLPC/cholesterol bilayers, and (*D*) Pyr_6PC and $Pyr_{14}PC$ in DOPC/7-SLPC/cholesterol bilayers. Each value represents an average of two to three experiments with three replicate samples. The error bars indicate the standard deviation.

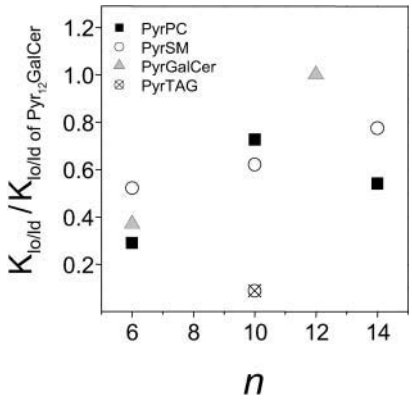

FIGURE 8 Relative l_o/l_d partition coefficients for pyrene lipids in BB-SM/7SLPC/cholesterol bilayers. The l_o/l_d partition coefficients ($K_{lo/ld}$) were determined by slope method described previously (Wang et al., 2000) and normalized relative to that of $Pyr_{12}GalCer$ and are plotted against the length of the pyrene-labeled acyl chain (n).

with this prediction (Fig. 7 *C*), i.e., the relative $K_{lo/ld}$ value obtained with the slope method was only 0.08 (Fig. 8).

DISCUSSION

Partition of the pyrene-labeled lipids between gel and liquid-crystalline domains

Both the *E/M* versus temperature and the quenching measurements indicated that partitioning of Pyr_nPC, Pyr_nSM, and $Pyr_nGalCer$ shifted in favor of the gel phase when the length of the labeled chain increased (Figs. 4 and 6). The quenching data gave much smaller values for $K_{g/f}$ than the *E/M* data. Notably, however, these values cannot be directly compared since 1), the highest melting subtransition of BB-SM ($T_m \sim 41°C$) was not considered in the analysis of the *E/M* data for practical reasons (see Results); 2), the temperature at which the partition coefficients were determined was different in the quenching and *E/M* vs. *T* experiments; and 3) the lipid compositions were also different (neat BB-SM vs. BB-SM/7-SLPC).

Why does the length of labeled acyl chain affect the partitioning of the pyrene lipid molecules? In this respect, it is notable that when the nominal length of the pyrene-labeled chain increases, two things happen simultaneously: 1), the effective length of the chain increases and 2), the pyrene moiety moves deeper into the bilayer (Sassaroli et al., 1995). Previous studies have shown that partitioning of lipids (or mimics) containing saturated alkyl chains to gel domains is maximal when the length of the alkyl chains is approximately equal to the length of the chains of the lipid forming the gel domains (Klausner and Wolf, 1980; Spink et al., 1990; Mesquita et al., 2000; Wang and Silvius, 2003). The length of a Pyr_6 acyl chain, including the pyrene moiety, equals to that of an alkyl chain with 11.5 carbon units (Sassaroli et al., 1995), and is thus much shorter than the estimated average length of BB-SM alkyl chains (~19–20 carbons). On the other hand, the total length of a Pyr_{14}acyl chain is ~19.5 carbon units and thus very similar to that of the BB-SM chains. Therefore, it is likely that the more avid partitioning of the long-chain pyrene lipids to the gel domains is, at least in part, due to that the length of their acyl chains better matches the length of the chains of the lipids forming those domains.

Regarding the effect of pyrene position in the bilayer, it is worthy to mention that the mean depth of the pyrene moiety attached to a phospholipid acyl chain has been shown to increase systematically with increasing length of the linked chain both in the presence and absence of cholesterol (Eklund et al., 1992; Sassaroli et al., 1995). On the other hand, it is known that in fluid BB-SM bilayers the acyl chains are more ordered, and thus more tightly packed together, close to bilayer surface (acyl carbons 1–10) as compared to the core region (Guo et al., 2002). Such transversal gradient of alkyl chain order is likely to be maintained to some degree also in the gel state due to heterogeneity of acyl chain length (16–24 carbons) and unsaturation (0–1 double bonds) of BB-SM. Thus, when the pyrene is attached to a short acyl chain ($n \leq 8$), it will partly reside in the more ordered region of the bilayer, which, due to bulkiness of pyrene, is expected to significantly perturb the packing of BB-SM acyl chains. When the length of the labeled chain increases, the pyrene moiety moves to the less ordered and less tightly packed core region of the bilayer where it is better accommodated than when it is closer to the bilayer surface. Previous studies have shown that addition of a double bond to a saturated acyl chain dramatically shifts the partitioning of the parent lipid or a lipid-like molecule in favor of the fluid phase (Welti and Silbert, 1982; Martin et al., 1990; Mesquita et al., 2000; Wang et al., 2000). A double bond causes the acyl chain to kink and thus perturbs packing of neighboring acyl chains similarly to a pyrene moiety.

Also the lipid backbone and headgroup structures were found to affect, albeit modestly, the distribution of pyrene lipids between gel and liquid-crystalline domains. Visual inspection of the *E/M* versus temperature curves indicates that Pyr_nPCs partition slightly more to the gel domains than Pyr_nSMs when the chain length is equal (Fig. 2). The $K_{g/f}$ values determined using the model described in Appendix 1 are consistent with this conclusion, albeit no significant differences were observed for all chain lengths (Fig. 4). One possible explanation for these data is that the pyrene moiety of Pyr_nSM is less deeply inserted in the bilayer than that of corresponding Pyr_nPC. Hoffmann and co-workers have recently proposed that a nitroxide moiety attached to the acyl chain of SM lies ~1 methylene unit closer to the membrane surface than when the same acyl is attached at the *sn*-2 position of PC (Hoffmann et al., 2000). These authors attributed this difference to different molecular conformations of SM and PC, as indicated by their crystal structures. An alternative explanation would be that the whole SM molecule is less deeply inserted in the bilayer than PC. SM contains a polar hydroxyl group and a double bond in the upper part of the sphingosine moiety. These are absent in PC and thus SM is more polar than PC containing comparable hydrocarbon chains.

Our data indicates that $Pyr_nGalCer$ has a somewhat higher affinity for the gel domains than either Pyr_nPC or Pyr_nSM when $n > 8$ (Figs. 4 and 6). This is consistent with the recent data obtained for lipids containing an indolylstearic acid residue (Wang and Silvius, 2003). The higher gel domain affinity of the $Pyr_nGalCer$ derivatives could derive from that these species are better accommodated in such closely packed systems due to their smaller headgroup (Kulkarni et al., 1995). However, the data of Wang and Silvius indicate that no simple relationship between the headgroup size and partitioning between fluid and gel domains may exist (Wang and Silvius, 2003).

As far as we are aware, there are no previous detailed studies on how the position of a fluorophore (or other bulky

group) along an acyl chain of a phospho- or sphingolipid affects the partitioning of the labeled lipid between coexisting gel/liquid domains. Beck and colleagues have studied partitioning of two PC species carrying a fluorescent diphenylhexatriene moiety attached either to a long (C_{22}) or a short (C_3) acyl chain between fluid and gel domains coexisting in dielaidoyl-PC/distearoyl-PC bilayers (Beck et al., 1993). They found that the long-chain probe preferred the gel domains whereas the short-chain probe preferred the fluid ones. Huang and co-workers studied the partitioning of anthroyloxy-labeled fatty acids between gel and fluid domains in DPPC or DSPC bilayers (Huang et al., 1988) and found that the probes partitioned preferentially and equally to the fluid domains ($K_{g/f} \approx 0.25$) when the position of the anthroyloxy moiety was varied between the carbons 3 and 12 of a stearic acid. Increased partitioning to the gel domains was observed when the probe was attached to the carbon 16 of a palmitic acid ($K_{g/f} \approx 0.7$). The fact that no effect on probe partitioning was observed until the fluorophore was placed beyond carbon 12 could be due to that in the gel-state DPPC and DSPC bilayers are conformationally more ordered than BB-SM bilayers studied here. In addition, a fatty acid could partition differently from complex lipids like PC and SM (see below).

Partition of pyrene lipids between liquid-ordered and liquid-disordered domains

Partitioning of pyrene lipids between l_o and l_d domains coexisting in BB-SM/7-SLPC/cholesterol bilayers was studied by using the quenching method. In this system, the l_o domains probably consist mainly of BB-SM and cholesterol, whereas the l_d domains consist mainly of 7-SLPC. The relative partition coefficients obtained show that, in general, the affinity for the l_o domains increases with the length of the pyrene-labeled chain (Fig. 8). However, Pyr_nPC is an exception since $Pyr_{14}PC$ partitioned less to the l_o domains than $Pyr_{10}PC$ at higher 7-SLPC mole fractions (Fig. 8). A possible explanation could be that in the l_o domains the pyrene moiety of $Pyr_{14}PC$ interacts unfavorably with the molecules in the opposite leaflet. Thus $Pyr_{14}PC$ would have a lower affinity for such domains than the species with a somewhat shorter chain, e.g., $Pyr_{10}PC$. The absence of such anomalous chain-length dependency in BB-SM/7-SLPC bilayers (Figs. 4 and 6) could relate to the fact that the SM gel domains are thicker than the SM/cholesterol l_o domains (Maulik and Shipley, 1996a,b) and thus the Pyr_{14} chain does not reach the opposite monolayer in BB-SM gel domains. These suggestions are consistent with studies carried out with other labeled lipids showing that an optimal chain-length exists for partitioning into l_o domains (Wang et al., 2000; Wang and Silvius, 2003). Notably, the fact that partitioning of Pyr_nSM to l_o domains increased with n with no anomaly (Fig. 8) could be due to a shallower position of the pyrene in these lipids as compared to Pyr_nPC with equal n (see above). However, it cannot be excluded that other factors as well, such as higher affinity of SM for cholesterol (Ramstedt and Slotte, 2002), play a role here.

Although the absolute partition coefficients could not be determined in this study, the shape of the quenching curves (Fig. 7) as well as the much lower relative $K_{lo/ld}$ value obtained for pyrene triglyceride (Fig. 8) indicate that the long-chain pyrene lipids partition preferentially to the l_o domains, whereas the short-chain ones prefer the l_d domains. Previously, phospho- and sphingolipids with another type of fluorophore attached to short acyl chain were found to partition largely into l_d domains (Wang and Silvius, 2000; Samsonov et al., 2001).

Beside the chain-length per se, the depth of pyrene in the bilayer could also influence domain partitioning, and this effect could be much more pronounced in the presence of cholesterol. Both pyrene and cholesterol have rigid and planar structures and thus their relative depths in the bilayer could have a marked effect on pyrene lipid partitioning to the cholesterol-rich l_o domains. The sign and magnitude of this effect are, however, difficult to estimate from the existing data. The headgroup also influenced the partitioning of pyrene lipids into l_o domains, since the partitioning of long-chain chain pyrene lipids to l_o domains increased in the order $PC < SM < GalCer$ (Fig. 8). This order agrees with that obtained previously for other fluorescent lipids (Wang and Silvius, 2000, 2003).

Implications on the use of pyrene lipids to study raft properties and intracellular lipid trafficking

One of the goals of this study was to estimate whether pyrene-labeled lipids could be used to detect and probe rafts or similar domains in cellular membranes. As was discussed above, the shape of the quenching curves indicates that long-chain pyrene lipids partition significantly to l_o domains. Consistent with this conclusion, we have recently found that when Pyr_nSM species were introduced to human fibroblasts and the cells were then exposed to Triton X-100 at 4°C, ~60% of $Pyr_{16}SM$ and ~35% of $Pyr_{12}SM$ was found in insoluble membrane fraction (as were ~60% of the natural SM species). In contrast, almost all of Pyr_4SM was found in the soluble fraction (unpublished data). These observations strongly suggest that long-chain pyrene lipids partition to rafts or similar domains in cellular membranes and could thus be used to probe these entities.

Pyrene lipids have been proven as useful tools to study intracellular lipid trafficking as was noted in the Introduction. For correct interpretation of the data obtained in such studies it is essential to understand the how the labeled lipids partition between the different domains existing in the various cellular membranes. This is because rafts are likely to play an important role in intracellular lipid sorting and trafficking (van Meer and Lisman, 2002). Strong experimental

evidence for domain partition-dependent sorting of lipids comes from a study showing that endocytic sorting of fluorescent lipids and mimics is determined by the length and unsaturation of their alkyl chains (Mukherjee et al., 1999). The differential partitioning of short- and long-chain pyrene lipids as found here could be used to further probe the role of membrane domains in intracellular lipid sorting and trafficking. The recently developed method of Tanhuanpää and Somerharju (1999) and Heikinheimo and Somerharju (2002) allowing the introduction of long-chain pyrene lipids to cells help to make such studies feasible.

Finally, it is worthy to mention that the lipid backbone and headgroup-specific properties do not seem to be severely masked by the pyrene moiety, as indicated by the fact that significant differences in partitioning were observed between Pyr_nPC, Pyr_nSM, and $Pyr_nGalCer$ classes. This conclusion is supported by previous data obtained for different glycerophospholipid classes (Somerharju et al., 1985).

APPENDIX 1. MODELING OF THE EXCIMER AND MONOMER FLUORESCENCE INTENSITY VERSUS TEMPERATURE PLOTS

The partitioning of the pyrene lipids between solid and fluid phases (domains) was analyzed based on a model assuming that 1), N solid phases with different compositions form sequentially in BB-SM bilayers upon cooling as indicated by the calorimetric analysis (cf. Fig. 1) and 2), that partitioning of a pyrene lipid molecule between each solid phase and coexisting liquid phase is defined by a unique partition coefficient. The partitioning coefficients can be determined from the temperature dependency of the excimer (E) and monomer (M) fluorescence intensities as follows.

The temperature dependence of the fractional area covered by a liquid phase n (λ_n) is described by a Hill equation as

$$\lambda_n = s_n \times \frac{T^c}{T^c + T^c_{m,n}}, \quad n = 1, 2 \ldots, N, \tag{1}$$

where s_n is the maximum of the fractional area covered by a solid phase n, c is the cooperativity of the transition (the Hill coefficient), and $T_{m,n}$ is the peak temperature of that transition. The solid fractional area of each component is

$$\sigma_n = s_n - \lambda_n, \quad n = 1, 2 \ldots, N. \tag{2}$$

A small yet significant fraction of the lipids may be in the liquid state even at the lowest temperature of measurement, i.e., 10°C. The area fraction occupied by those molecules is denoted by λ_0. Since three solids and one fluid phase can exist in this system, the total fractional area covered by the liquid phase (λ) is

$$\lambda = \lambda_0 + \lambda_1 + \ldots \lambda_N = \sum_{n=0}^{N} \lambda_n. \tag{3}$$

The total excimer fluorescence intensity is

$$E_{Tot} = x_l \times \lambda \times E_l(x_l, T) + \sum_{n=1}^{N} x_{s,n} \times \sigma_n \times E_s(x_n, T), \tag{4}$$

where x_l and $x_{s,n}$ represent the concentrations of the labeled lipid in the fluid phase and each solid phase, and E_l and E_s indicate the fluid and solid phase contributions to the excimer fluorescence, respectively. It is further assumed that

$$E_l(x_l, T) = f_{E_l}(T) \times Pol_{E_l}(x_l) \tag{5a}$$

and

$$E_s(x_{s,n}, T) = f_{E_s}(T) \times Pol_{E_s}(x_{s,n}), \tag{5b}$$

where $f_{E_l}(T)$ and $f_{E_s}(T)$ are exponential functions describing the temperature dependencies of the excimer fluorescence intensity in the liquid and solid domains, respectively, and $Pol_{E_l}(x_l)$ and $Pol_{E_s}(x_{s,n})$ are polynomials describing the probe concentration dependency of the excimer fluorescence intensities when the bilayer is fully in the liquid ($T = 50$°C) or solid ($T = 10$°C) states, respectively. The temperature dependency of excimer formation in the fluid and solid phases are described by $f_{E_l}(T)$ and $f_{E_s}(T)$, respectively, and are defined as

$$f_{E_l}(T) = e^{B_{E_l}\left(\frac{T-50}{T+273}\right)} \tag{6a}$$

and

$$f_{E_s}(T) = e^{B_{E_s}\left(\frac{T-10}{T+273}\right)}, \tag{6b}$$

where $B_{E_l} = (\Delta E^*_{E_l}/k \cdot 323)$ and $B_{E_s} = (\Delta E^*_{E_s}/k \cdot 283)$, k is the Boltzmann constant, and $\Delta E^*_{E_l}$ and $\Delta E^*_{E_s}$ indicate the activation energies for excimer formation in the liquid and solid phases, respectively. The parameters of the third-degree polynomials, $Pol_{E_s}(x_s)$ and $Pol_{E_l}(x_l)$, were determined by measuring the excimer intensity as a function of pyrene lipid mole fraction at 10°C and 50°C, respectively.

Analogously, the total *monomer* intensity is defined by the equation

$$M_{Tot} = x_l \times \lambda \times M_l(x_l, T) + \sum_{n=1}^{N} x_{s,n} \times \sigma_n \times M_s(x_{s,n}, T), \tag{7}$$

where the symbols are analogous to those given above for the total excimer fluorescence. Finally, the concentrations of the probe in the different phases can be coupled by the following equation

$$x_0 = \lambda \times x_l + \sum_{n=1}^{N} \sigma_n \times x_{s,n}. \tag{8}$$

Notably, we also tested an alternative model that included the domain boundaries. However, this did not improve the fits, indicating that the probes do not have a strong tendency to concentrate to the boundaries and therefore it is not useful to employ such a more complex model here.

APPENDIX 2. MODELING OF PYRENE LIPID FLUORESCENCE QUENCHING

The framework of these calculations is given in Fig. 9. To simplify the visualization as well as some calculations, it was assumed that the packing symmetry of phospholipid molecules is hexagonal and that the quencher domains are hexagonal as well. Notably, however, the analysis can be readily generalized to apply to other domain shapes and packing symmetries, including totally random packing as will be shown elsewhere (unpublished data).

By denoting the radius of the quencher domains by q, the length of the quencher domain perimeter will the be $6q$ and its area $3q(q + 1) + 1$. Since the unit here is a molecule, the area equals the number of molecules in the domain. For the purpose of calculations, the area surrounding the quencher domain is divided into molecular shells. The first shell ($n + 1$) consists of the molecules in direct contact with the quencher domain (part of these are shown in *shaded representation* in Fig. 9), the second shell consists of the molecules outside the first shell, etc.

To calculate the quenching probability one needs to determine the fraction of excited molecules that come in contact with the quenching domain, i.e., reach the first shell during their excitation lifetime. In this analysis it is assumed that the molecular movement takes place in distinct

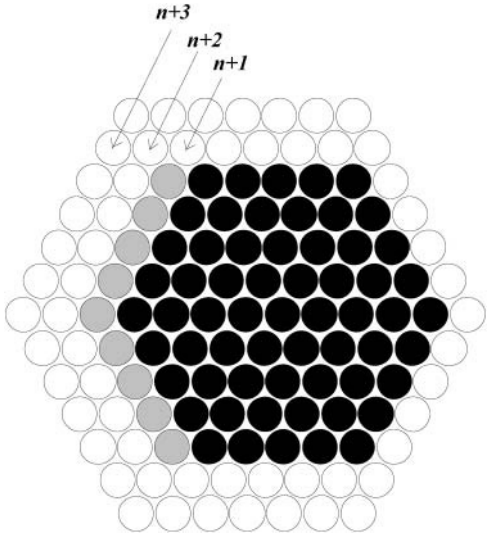

FIGURE 9 The framework used to model pyrene lipid quenching by quencher lipid domains. The open and solid circles represent the unlabeled lipid and quencher lipid molecules, respectively. Some unlabeled lipid molecules residing in the molecular shell next to the quencher domain ($n + 1$) are shown in shaded representation. See the text for other details.

jumps between layers and that the time needed for one jump is constant. Then, the fraction of excited (fluorescent) molecules remaining after one jump, [P^*], will be

$$[P^*] = [P^*]_0 e^{-\frac{\tau_R}{\tau_F}} = [P^*]_0 e_\tau, \tag{9}$$

where τ_R is the residence time, τ_F is the fluorescence lifetime of the excited molecule, and $[P^*]_0$ is the mole fraction of excited molecules before the jump. The probability for a molecule to move from one shell to another is directly proportional to the length of the border between those shells and thus the quenching probability of a molecule in the second shell (Q_{21}) is

$$Q_{21} = \frac{2q+3}{6(q+2)} e_\tau + \frac{1}{3} e_\tau Q_{21} + \frac{2q+5}{6(q+2)} e_\tau Q_{31}. \tag{10}$$

The first term describes the probability that the molecule jumps directly to the first shell, the second term accounts for molecules that stay in the second shell but will enter the first shell later on (with the probability Q_{21}), whereas the third term accounts for molecules that first jump to the third shell but (with probability Q_{31}) enter the first shell later. Likewise, the quenching probability of a molecule located in the third shell (Q_{31}) is

$$Q_{31} = Q_{32} \times Q_{21}, \tag{11}$$

where Q_{32} is the probability that such a molecule enters the second shell, and Q_{21} is as defined above. Finally, it can be shown that the total number of quenched molecules ($M_{N,1}$) in the shells 1–N is given by the following equation,

$$M_{N,1} = 6\left\{\sum_{n=2}^{N}(q+n)(f_\tau)^{n-1}\prod_{j=2}^{n}\left[1-\frac{1}{2(q+j)}\right]\right\}[P^*]_0, \tag{12}$$

where

$$f_\tau = \frac{1}{2e_\tau}\left[3 - e_\tau - \sqrt{3(1-e_\tau)(3+e_\tau)}\right].$$

Equation 4 can thus be expressed briefly as

$$M_{N,1} = k_{dom}[P^*]_0, \tag{13}$$

where k_{dom}, the domain quenching constant, is a function of the quencher domain size (q), the fluorescence lifetime (τ_F), and the residence time (τ_R) of the probe. When the quencher domains are small, one also has to take their diffusion into account; i.e., a reduced residence time needs to be used,

$$\frac{1}{\tau_{R,eff}} = \frac{1}{\tau_R} + \frac{1}{\sqrt{3q(q+1)+1}\cdot\tau_R}. \tag{14}$$

The effective diffusion coefficient ($1/\tau_{R,eff}$) is thus equal to the sum of the diffusion coefficients of the fluorophore and the quencher domains, as in the case of molecular quenchers (cf. Lacowicz, 1983). The fluorescence intensity is proportional to the total number of excited molecules according to

$$F \propto a_N \times [P^*]_0 - k_{dom} \times [P^*]_0, \tag{15}$$

where the first term gives the number of excited molecules in the area a_N surrounding a quencher domain and the second term indicates the number of excited molecules that will be actually quenched. In the absence of the quencher $F_0 \propto a_N \cdot [P^*]_0$, the relative fluorescence F_R measured in the presence of the quencher lipid is

$$F_R = \frac{F}{F_0} = 1 - \frac{k_{dom}}{a_N} = 1 - \frac{k_{dom}}{a_Q}\frac{a_Q}{a_N} = 1 - \frac{k_{dom}}{a_Q}x_Q, \tag{16}$$

where x_Q is the quencher mole fraction and a_Q is the area of the quencher domain expressed as the number of molecules. Notably, the standard Stern-Volmer equation relating the relative fluorescence intensity to the quencher concentration is (Lacowicz, 1983)

$$F_R = \frac{1}{1 + k_Q \times x_Q} \approx 1 - k_Q \times x_Q. \tag{17}$$

The approximation is valid at low quencher concentrations. By comparing Eqs. 7 and 8 one can note that

$$k_Q = \frac{k_{dom}}{a_Q}, \tag{18}$$

if the quencher domains consist of single quencher molecules, $k_{dom} = k_{mon}$, $a_Q = 1$, and $k_Q = k_{mon}$. Thus, we have established the relationship between the quenching rate constant and the size of the quencher domain. Although this result was derived for low quencher concentrations, the quenching constant can be assumed to be (nearly) constant over the whole concentration range.

We are grateful to Ms. Tarja Grundström for skillful technical assistance, Ms. Jenni Tamminen for help with various assays, and Dr. Andreas Uphoff and Martin Hermansson, MSc, for critical reading of the manuscript.

REFERENCES

Agmon, V., T. Dinur, S. Cherbu, A. Dagan, and S. Gatt. 1991. Administration of pyrene lipids by receptor-mediated endocytosis and their degradation in skin fibroblasts. *Exp. Cell Res.* 196:151–157.

Ahmad, T. Y., J. T. Sparrow, and J. D. Morrisett. 1985. Fluorine-, pyrene-, and nitroxide-labeled sphingomyelin: semi-synthesis and thermotropic properties. *J. Lipid Res.* 26:1160–1165.

Ahmed, S. N., D. A. Brown, and E. London. 1997. On the origin of sphingolipid/cholesterol-rich detergent-insoluble cell membranes: physiological concentrations of cholesterol and sphingolipid induce formation of a detergent-insoluble, liquid-ordered lipid phase in model membranes. *Biochemistry.* 36:10944–10953.

Almeida, P. F., W. L. Vaz, and T. E. Thompson. 1992. Lateral diffusion in the liquid phases of dimyristoylphosphatidylcholine/cholesterol lipid bilayers: a free volume analysis. *Biochemistry.* 31:6739–6747.

Anderson, R. G., and K. Jacobson. 2002. A role for lipid shells in targeting proteins to caveolae, rafts, and other lipid domains. *Science*. 296:1821–1825.

Barenholz, Y., J. Suurkuusk, D. Mountcastle, T. E. Thompson, and R. L. Biltonen. 1976. A calorimetric study of the thermotropic behavior of aqueous dispersions of natural and synthetic sphingomyelins. *Biochemistry*. 15:2441–2447.

Bartlett, E. M., and D. H. Lewis. 1970. Spectrophotometric determination of phosphate esters in the presence and absence of orthophosphate. *Anal. Biochem*. 36:159–167.

Beck A., D. Heissler, and G. Duportail. 1993. Influence of the length of the spacer on the partitioning properties of amphiphilic fluorescent membrane probes. *Chem. Phys. Lipids*. 66:135–142.

Brown, D. A., and E. London. 2000. Structure and function of sphingolipid- and cholesterol-rich membrane rafts. *J. Biol. Chem*. 275:17221–17224.

Calhoun, W. I., and G. G. Shipley. 1979. Fatty acid composition and thermal behavior of natural sphingomyelins. *Biochim. Biophys. Acta*. 555:436–441.

Chong, P. L., and T. E. Thompson. 1985. Oxygen quenching of pyrene-lipid fluorescence in phosphatidylcholine vesicles. A probe for membrane organization. *Biophys. J*. 47:613–621.

Edidin, M. 2003. The state of lipid rafts: from model membranes to cells. *Annu. Rev. Biophys. Biomol. Struct*. 16:16.

Eklund, K. K., J. A. Virtanen, P. K. Kinnunen, J. Kasurinen, and P. J. Somerharju. 1992. Conformation of phosphatidylcholine in neat and cholesterol-containing liquid-crystalline bilayers. Application of a novel method. *Biochemistry*. 31:8560–8565.

Galla, H. J., and E. Sackmann. 1975. Chemically induced phase separation in mixed vesicles containing phosphatidic acid. An optical study. *J. Am. Chem. Soc*. 97:4114–4120.

Guo, W., V. Kurze, T. Huber, N. H. Afdhal, K. Beyer, and J. A. Hamilton. 2002. A solid-state NMR study of phospholipid-cholesterol interactions: sphingomyelin-cholesterol binary systems. *Biophys. J*. 83:1465–1478.

Heikinheimo, L., and P. Somerharju. 2002. Translocation of pyrene-labeled phosphatidylserine from the plasma membrane to mitochondria diminishes systematically with molecular hydrophobicity: implications on the maintenance of high phosphatidylserine content in the inner leaflet of the plasma membrane. *Biochim. Biophys. Acta*. 1591:75–85.

Hoffmann, P., K. Sandhoff, and D. Marsh. 2000. Comparative dynamics and location of chain spin-labelled sphingomyelin and phosphatidylcholine in dimyristoyl phosphatidylcholine membranes studied by EPR spectroscopy. *Biochim. Biophys. Acta*. 1468:359–366.

Hresko, R. C., I. P. Sugar, Y. Barenholz, and T. E. Thompson. 1986. Lateral distribution of a pyrene-labeled phosphatidylcholine in phosphatidylcholine bilayers: fluorescence phase and modulation study. *Biochemistry*. 25:3813–3823.

Hresko, R. C., I. P. Sugar, Y. Barenholz, and T. E. Thompson. 1987. The lateral distribution of pyrene-labeled sphingomyelin and glucosylceramide in phosphatidylcholine bilayers. *Biophys. J*. 51:725–733.

Huang, N. N., K. Florine-Casteel, G. W. Feigenson, and C. Spink. 1988. Effect of fluorophore linkage position of *n*-(9-anthroyloxy) fatty acids on probe distribution between coexisting gel and fluid phospholipid phases. *Biochim. Biophys. Acta*. 939:124–130.

Ipsen, J. H., G. Karlstrom, O. G. Mouritsen, H. Wennerstrom, and M. J. Zuckermann. 1987. Phase equilibria in the phosphatidylcholine-cholesterol system. *Biochim. Biophys. Acta*. 905:162–172.

Jones, M. E., and B. R. Lentz. 1986. Phospholipid lateral organization in synthetic membranes as monitored by pyrene-labeled phospholipids: effects of temperature and prothrombin fragment 1 binding. *Biochemistry*. 25:567–574.

Kasurinen, J., and P. Somerharju. 1995. Metabolism and distribution of intramolecular excimer-forming dipyrenebutanoyl glycerophospholipids in human fibroblasts. Marked resistance to metabolic degradation. *Biochemistry*. 34:2049–2057.

Klausner, R. D., and D. E. Wolf. 1980. Selectivity of fluorescent lipid analogues for lipid domains. *Biochemistry*. 19:6199–6203.

Koivusalo, M., P. Haimi, L. Heikinheimo, R. Kostiainen, and P. Somerharju, P. 2001. Quantitative determination of phospholipid compositions by mass spectrometry, effects of acyl chain length, unsaturation and lipid concentration on instrument response. *J. Lipid. Res*. 42:663–672

Kulkarni, V. S., W. H. Anderson, and R. E. Brown. 1995. Bilayer nanotubes and helical ribbons formed by hydrated galactosylceramides: acyl chain and headgroup effects. *Biophys. J*. 69:1976–1986.

Lacowicz, J. 1983. Principles of Fluorescence Spectroscopy. Plenum Press, New York.

London, E., and G. W. Feigenson. 1981a. Fluorescence quenching in model membranes. 1. Characterization of quenching caused by a spin-labeled phospholipid. *Biochemistry*. 20:1932–1938.

London, E., and G. W. Feigenson. 1981b. Fluorescence quenching in model membranes: an analysis of the local phospholipid environment of diphenylhexatriene and gramicidin A′. *Biochim. Biophys. Acta*. 649: 89–97.

Martin, L. R., R. B. Avery, and R. Welti. 1990. Partition of parinaroylphosphatidylethanolamines and parinaroylphosphatidylglycerols in immiscible phospholipid mixtures. *Biochim. Biophys. Acta*. 1023:383–388.

Masserini, M., A. Giuliani, P. Palestini, D. Acquotti, M. Pitto, V. Chigorno, and G. Tettamanti. 1990. Association to HeLa cells and surface behavior of exogenous gangliosides studied with a fluorescent derivative of GM1. *Biochemistry*. 29:697–701.

Maulik, P. R., and G. G. Shipley. 1996a. Interactions of *n*-stearoyl sphingomyelin with cholesterol and dipalmitoylphosphatidylcholine in bilayer membranes. *Biophys. J*. 70:2256–2265.

Maulik, P. R., and G. G. Shipley. 1996b. *N*-palmitoyl sphingomyelin bilayers: structure and interactions with cholesterol and dipalmitoylphosphatidylcholine. *Biochemistry*. 35:8025–8034.

Maxfield, F. R. 2002. Plasma membrane microdomains. *Curr. Opin. Cell Biol*. 14:483–487.

Mesquita, R. M., E. Melo, T. E. Thompson, and W. L. Vaz. 2000. Partitioning of amphiphiles between coexisting ordered and disordered phases in two-phase lipid bilayer membranes. *Biophys. J*. 78:3019–3025.

Mukherjee, S., T. T. Soe, and F. R. Maxfield. 1999. Endocytic sorting of lipid analogues differing solely in the chemistry of their hydrophobic tails. *J. Cell Biol*. 144:1271–1284.

Ollmann, M., G. Schwarzmann, K. Sandhoff, and H. J. Galla. 1987. Pyrene-labeled gangliosides: micelle formation in aqueous solution, lateral diffusion, and thermotropic behavior in phosphatidylcholine bilayers. *Biochemistry*. 26:5943–5952.

Pownall, H. J., and L. C. Smith. 1989. Pyrene-labeled lipids: versatile probes of membrane dynamics in vitro and in living cells. *Chem. Phys. Lipids*. 50:191–211.

Ramstedt, B., and J. P. Slotte. 2002. Membrane properties of sphingomyelins. *FEBS Lett*. 531:33–37.

Samsonov, A. V., I. Mihalyov, and F. S. Cohen. 2001. Characterization of cholesterol-sphingomyelin domains and their dynamics in bilayer membranes. *Biophys. J*. 81:1486–1500.

Sankaram, M. B., and T. E. Thompson. 1990. Interaction of cholesterol with various glycerophospholipids and sphingomyelin. *Biochemistry*. 29:10670–10675.

Sassaroli, M., M. Ruonala, J. Virtanen, M. Vauhkonen, and P. Somerharju. 1995. Transversal distribution of acyl-linked pyrene moieties in liquid-crystalline phosphatidylcholine bilayers. A fluorescence quenching study. *Biochemistry*. 34:8843–8851.

Schroeder, R., E. London, and D. Brown. 1994. Interactions between saturated acyl chains confer detergent resistance on lipids and glycosylphosphatidylinositol (GPI)-anchored proteins: GPI-anchored proteins in liposomes and cells show similar behavior. *Proc. Natl. Acad. Sci. USA*. 91:12130–12134.

Schroeder, R. J., S. N. Ahmed, Y. Zhu, E. London, and D. A. Brown. 1998. Cholesterol and sphingolipid enhance the Triton X-100 insolubility of glycosylphosphatidylinositol-anchored proteins by promoting the forma-

tion of detergent-insoluble ordered membrane domains. *J. Biol. Chem.* 273:1150–1157.

Silversand, C., and C. Haux. 1997. Improved high-performance liquid chromatographic method for the separation and quantification of lipid classes: application to fish lipids. *J. Chromatogr. B Biomed. Sci. Appl.* 703:7–14.

Silvius, J. R. 1992. Cholesterol modulation of lipid intermixing in phospholipid and glycosphingolipid mixtures. Evaluation using fluorescent lipid probes and brominated lipid quenchers. *Biochemistry.* 31:3398–3408.

Silvius, J. R. 2003. Role of cholesterol in lipid raft formation: lessons from lipid model systems. *Biochim. Biophys. Acta.* 1610:174–183.

Simons, K., and R. Ehehalt. 2002. Cholesterol, lipid rafts, and disease. *J. Clin. Invest.* 110:597–603.

Simons, K., and E. Ikonen. 1997. Functional rafts in cell membranes. *Nature.* 387:569–572.

Somerharju, P. 2002. Pyrene-labeled lipids as tools in membrane biophysics and cell biology. *Chem. Phys. Lipids.* 116:57–74.

Somerharju, P. J., D. van Loon, and K. W. Wirtz. 1987. Determination of the acyl chain specificity of the bovine liver phosphatidylcholine transfer protein. Application of pyrene-labeled phosphatidylcholine species. *Biochemistry.* 26:7193–7199.

Somerharju, P. J., J. A. Virtanen, K. K. Eklund, P. Vainio, and P. K. Kinnunen. 1985. 1-Palmitoyl-2-pyrenedecanoyl glycerophospholipids as membrane probes: evidence for regular distribution in liquid-crystalline phosphatidylcholine bilayers. *Biochemistry.* 24:2773–2781.

Spink, C. H., M. D. Yeager, and G. W. Feigenson. 1990. Partitioning behavior of indocarbocyanine probes between coexisting gel and fluid phases in model membranes. *Biochim. Biophys. Acta.* 1023:25–33.

Tanhuanpää, K., and P. Somerharju. 1999. gamma-cyclodextrins greatly enhance translocation of hydrophobic fluorescent phospholipids from vesicles to cells in culture. Importance of molecular hydrophobicity in phospholipid trafficking studies. *J. Biol. Chem.* 274:35359–35366.

van Meer, G., and Q. Lisman. 2002. Sphingolipid transport: rafts and translocators. *J. Biol. Chem.* 277:25855–25858.

Wang, T. Y., R. Leventis, and J. R. Silvius. 2000. Fluorescence-based evaluation of the partitioning of lipids and lipidated peptides into liquid-ordered lipid microdomains: a model for molecular partitioning into ''lipid rafts''. *Biophys. J.* 79:919–933.

Wang, T. Y., and J. R. Silvius. 2000. Different sphingolipids show differential partitioning into sphingolipid/cholesterol-rich domains in lipid bilayers. *Biophys. J.* 79:1478–1489.

Wang, T. Y., and J. R. Silvius. 2003. Sphingolipid partitioning into ordered domains in cholesterol-free and cholesterol-containing lipid bilayers. *Biophys. J.* 84:367–378.

Welti, R., and D. F. Silbert. 1982. Partition of parinaroyl phospholipid probes between solid and fluid phosphatidylcholine phases. *Biochemistry.* 21:5685–5689.

Viani, P., C. Galimberti, S. Marchesini, G. Cervato, and B. Cestaro. 1988. *N*-pyrene dodecanoyl sulfatide as membrane probe: a study of glycolipid dynamic behavior in model membranes. *Chem. Phys. Lipids.* 46:89–97.

Vist, M. R., and J. H. Davis. 1990. Phase equilibria of cholesterol/dipalmitoylphosphatidylcholine mixtures: 2H nuclear magnetic resonance and differential scanning calorimetry. *Biochemistry.* 29:451–464.

Xu, X., and E. London. 2000. The effect of sterol structure on membrane lipid domains reveals how cholesterol can induce lipid domain formation. *Biochemistry.* 39:843–849.